Available online at www.sciencedirect.com
ScienceDirect
Journal of Power Sources 180 (2008) 476–483
JOURNAL OF POWER SOURCES
www.elsevier.com/locate/jpowsour

Effects of operating conditions on the performances of individual cell and stack of PEM fuel cell

Jer-Huan Jang [a], Han-Chieh Chiu [a], Wei-Mon Yan [b,*], Wei-Lian Sun [b]

[a] *Department of Mechanical Engineering, Technology and Science Institute of Northern Taiwan, Beitou, Taipei 112, Taiwan, ROC*
[b] *Department of Mechatronic Engineering, Huafan University, Shih Ting, Taipei 223, Taiwan, ROC*

Received 21 December 2007; received in revised form 1 February 2008; accepted 1 February 2008
Available online 12 February 2008

Abstract

In this study, experiments were carried out to study the effects on the performances of individual cell and stack of PEM fuel cell. In the experiment, there are four key operating conditions that affect the cell performance, and they are gas humidification temperature, cell temperature, assembled torsion, and gas flow rate. A 5-cell stack of PEMFC was used to measure the voltage and current density for individual cell in this experiment. Results reveal that the performances of the center fuel cells are relatively lower than those of the cells on both sides of the stack. It is also shown that stack performance increases with the increase in the anode humidification temperature as well as the center cell of the stack. As for the effect of cell temperature, results indicate that stack performance increases with the increase in cell temperature. It is also disclosed that the performances of individual cell and stack do not change with the increase in the anode gas stoichiometric ratio, but increase with the increase in the cathode gas stoichiometric ratio. In addition, the experiment results also show that the whole stack's performance is enhanced with the increase in the assembling torsion.

Keywords: Fuel cell stack; Individual cell performance; Stoichiometric ratio

1. Introduction

Substantial efforts have been made to create inexpensive and efficient proton-exchange membrane fuel cell (PEMFC) during the past decades, owing to its higher energy efficiency, low pollution and low noise. There are lots of works [1–6] expended on development of numerical modeling in the 1990s. Current development for numerical analysis is in the direction of applying computational fluid dynamics (CFD) to solve the transport equations in PEM fuel cell [7–12].

However, practical applications require a fuel cell stack working at high current and voltage. Sufficient reactant gas is necessary for each cell in a stack in order to attain high performance and stable operation of cell stack. The research and development of fuel cell stack have received much attention due to the complexity of electrochemical process within fuel cell stack [13–16]. The operation conditions of cell stacks, cell temperature, gas humidification temperature, and gas flow rate may lead to an increase and/or decrease of stack performance. Mennola et al. [17] measured the ohm resistance and voltage for each single cell in the stack using the current interruption method. They found that the ohm resistances of the cells on both ends of the stack are higher than those of the cells near the center of the stack due to lower temperatures. Giddey et al. [18] studied a 15-cell stack with the power of 1 kW as the current was 110 A and 120 A respectively. Results showed that the voltages of the cells at two sides of stack are higher than those of the cells near the center and the voltage differences between individual cells would be enlarged with an increase of the current. Zhu et al. [19] experimentally investigated 10 different stacks with each made of 47 cells. In their study, it was disclosed that that the voltage of the end cells dropped down seriously.

Rodatz et al. [20] investigated some aspects critical to the operation of large fuel cell stacks in automotive applications such as control issues in the supply system, stack failures, and the appropriate counter measures as well as some procedures to increase the voltage stability. They pointed out four reasons which caused a mal-distribution of each single cell in a cell

* Corresponding author.
E-mail address: wmyan@huafan.hfu.edu.tw (W.-M. Yan).

0378-7753/$ – see front matter © 2008 Elsevier B.V. All rights reserved.
doi:10.1016/j.jpowsour.2008.02.001

Nomenclature

I	current density (mA/cm^2)
V	voltage (V)
T_A	anode humidification temperature (°C)
T_C	cathode humidification temperature (°C)
T_{Cell}	stack temperature (°C)
λ_A	gas stoichiometric ratio in anode
λ_C	gas stoichiometric ratio in cathode
τ	assembling torsion (lb in)

Subscript

A	anode
C	cathode
Cell	stack

stack: 1, insufficient fuel supply and negative voltage; 2, fracture of the membrane; 3, overheating; 4, huge differential pressure. Sohn et al. [21] analyzed the operating conditions affecting the performance of an air-cooling PEMFC which is designed for portable applications. In this study a 500 W air-cooling PEMFC was fabricated and tested to evaluate the design performance and to determine optimal operating conditions. They showed that the stress caused by the pressure drop was enough to remove the excessive water in the stack when relative humidity (RH) was between 50% and 70%. However, an extremely high RH (RH > 70%) would cause water flooding phenomena, when the amount of water generated in the cell was larger than that was removed, leading to a corresponding degradation of the cell. Tanaka et al. [22] developed a method to stabilize a PEFC stack output and clarified operating conditions that affect the I–V characteristic curve, including stack-operating temperature (coolant outlet temperature), gas operating pressure, gas utilization ratio (gas stoichiometry), and gas dew point. Chu and Jiang [23] evaluated the performance of an air-breathing PEMFC stack under different environmental conditions. It was found that the humidity of the surrounding air significantly affected the performance of the stack. When the humidity was less than 10% RH at 35 °C, the stack lost almost 95% in power.

Proper gas and water management are essential to achieving and maintaining high power output in a PEM fuel cell stack. Knobbe et al. [24] employed the active gas management system controlling gas flow rate in each single cell to study the performance in small and large air cathode stacks of five and six cells. They demonstrated that both large and small stack received a 30% power increase after accounting for parasitic losses. Recently, Yan et al. [25] presents the AC impedance characteristics of a 2 kW PEMFC stack under different operating conditions and load charges. They showed that air stoichiometry, air humidity, and operation temperature have significant effects on the AC impedance of stack.

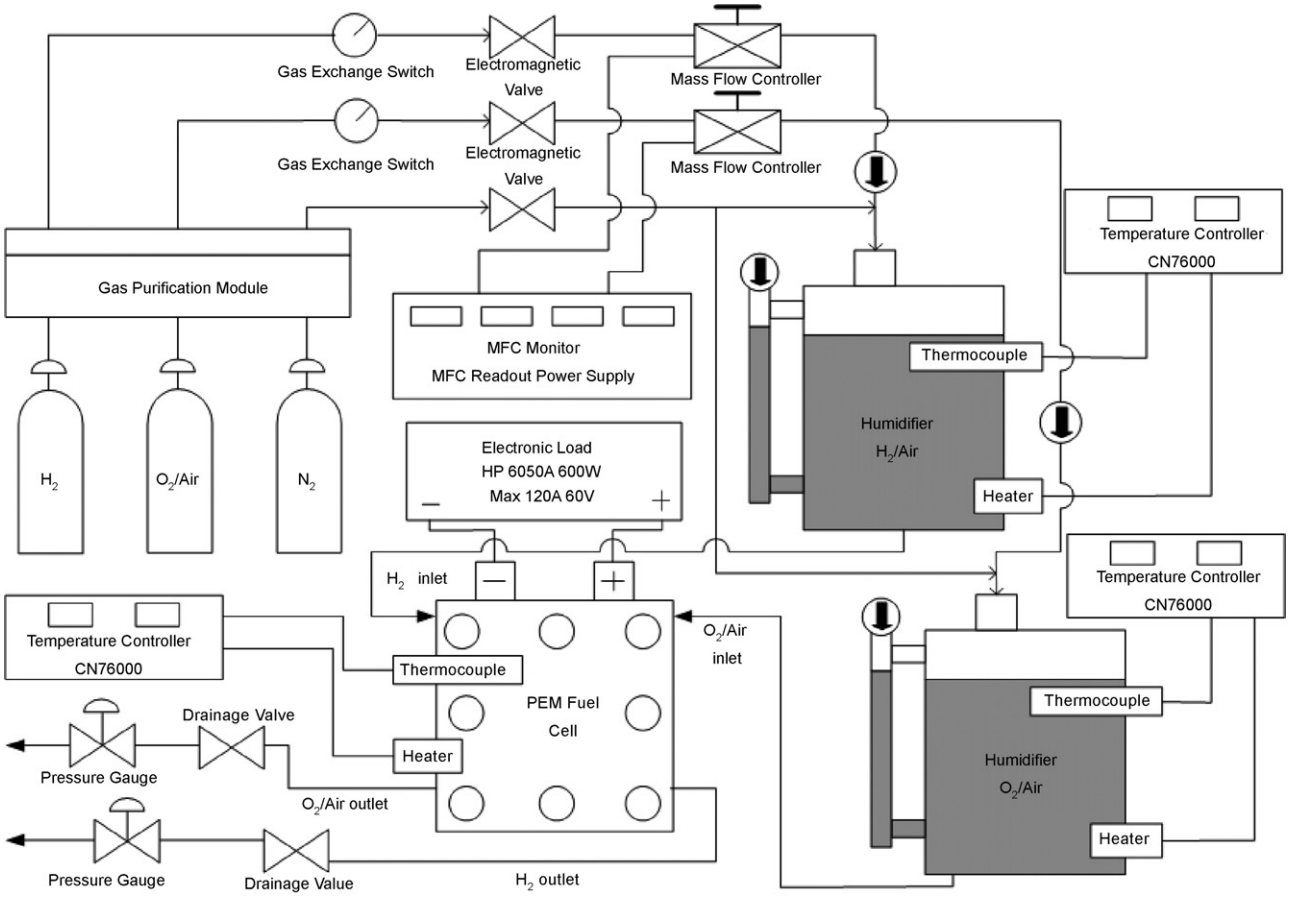

Fig. 1. Schematic diagram of the testing system.

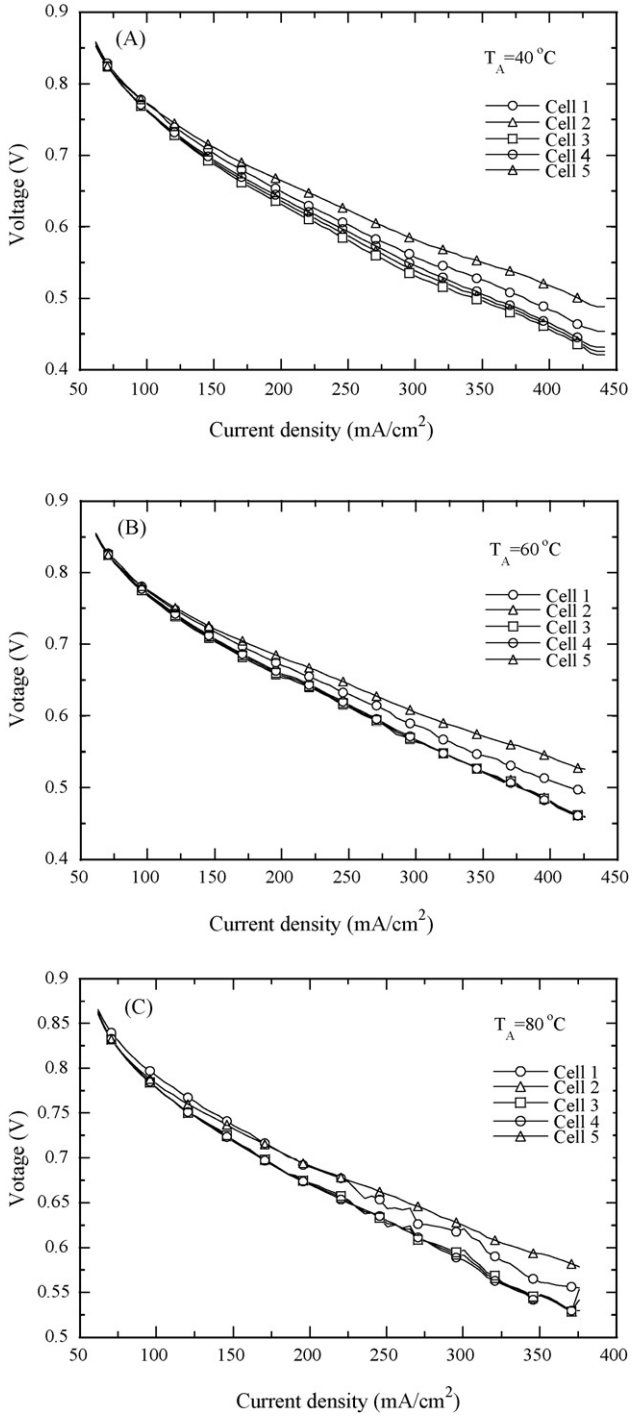

Fig. 2. Effect of anode gas humidification temperature on the performance of each single cell in the stack; (A) 40 °C; (B) 60 °C; (C) 80 °C.

From the literatures cited above, it is noticed that not only the operation parameters but also some design, material and assembly aspects might have some influence on the stack's performance. Apparently, the effects of operation conditions on the performance of individual fuel cell in a cell stack are key issues. The main purpose of this work is to investigate the performances of individual cell and cell stack through changing these operation parameters.

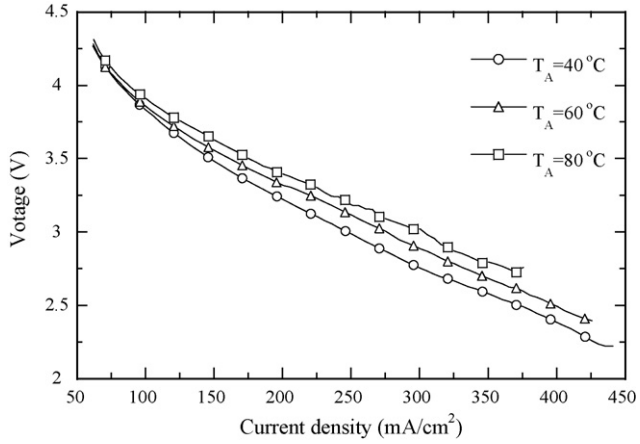

Fig. 3. Effects of anode gas humidification temperature on the overall performance of the stack.

2. Experiment

The membrane electrode assembly (MEA) used in the present experiment is produced by GORE with active surface area of $10 \times 10\,cm^2$. The catalyst Pt loading is $1.4\,mg/cm^2$ in the anode and $2\,mg/cm^2$ in the cathode. The material for the Gas Diffuser Layer (GDL) is the carbon paper produced by GORE-TEX with the thickness of 0.4 mm and the area of 13.5 cm × 13.5 cm. The bipolar plate is highly dense carbon plate produced by POCO. Its pattern number is AXF-5QCF with a size of 13.5 cm × 13.5cm and 3 mm in width. The distribution channels are machined as a 5-inlet and 5-outlet designed serpentine flow field with a rectangular shape on the polar plate. The width and depth of the channels are both 1 mm for a distribution area of $10 \times 10\,cm^2$. The current collector is made of copper, on which a gold layer was overlaid to reduce the contact resistance and to enhance erosion resistance between the two plates. The dimension of the current collector is $13.5 \times 13.5\,cm^2$ with thickness of 3 mm. As for the end plate, it is made of stainless steel with the area of $18.9 \times 18.9\,cm^2$ and 30 mm in thickness.

The physical system used in the experiment is shown in Fig. 1. It is a fuel cell testing system made by ARBIN Co. This apparatus consists of a gas supply system, a flow control system, a temperature control system, a humidification system, a load system and a computerized DAQ system. The internal structure of this apparatus includes: 1, temperature control system and temperature measuring devices; 2, humidity control system; 3, gas supply system; and 4, electric load system. The operating temperature ranged from 25 to 100 °C, with two inflow type: Hydrogen/oxygen and hydrogen/air. A heater with an Omega CN76000 PID temperature controller is employed to heat the PEM stack to the desired temperature. There is coolant flow through the stack for each individual cell. The gas supplied manifold has been designed in order that the supplied gas flows to each individual cell uniformly. A flow simulation has also been carried on to assure a uniform flow with the manifold.

The voltage of a single cell in the stack is measured by the device of Model 139326_AUX_IO_VI_300V_64CH produced by Arbin Co. This apparatus can measure at most 32 cells' voltage

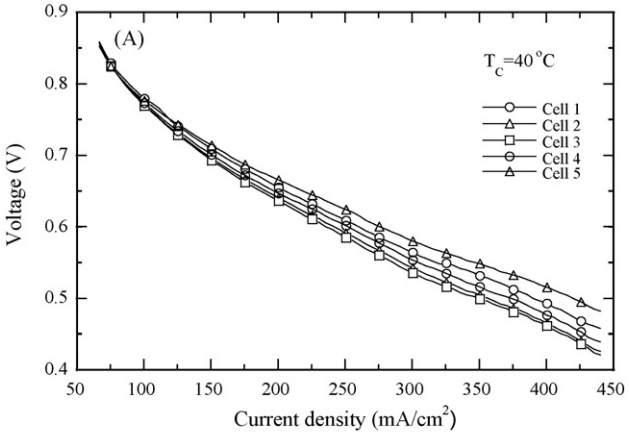

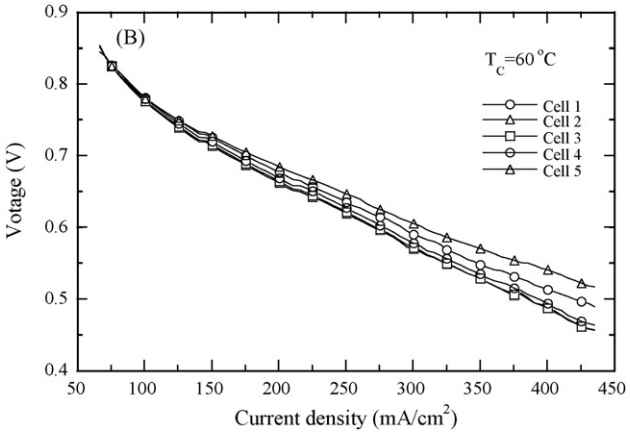

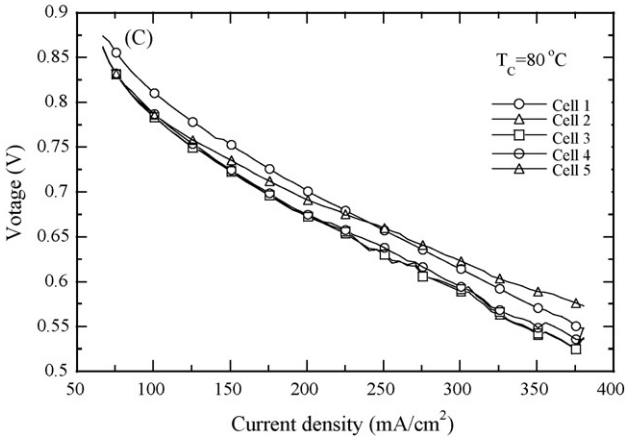

Fig. 4. Effect of cathode gas humidification temperature on the performance of each single cell's in the stack (A) 40 °C; (B) 60 °C; (C) 80 °C.

and thereby has 64 channels, which are connected on the cathode and anode side. Since the operating voltage of the cell is between 0 and 1 V, it is enough to satisfy voltage output for each single cell when the measurement range of the system is set as 0–2 V.

3. Results and discussion

In the present experimental study, cell performances for individual fuel cell and stack are measured. The conditions for

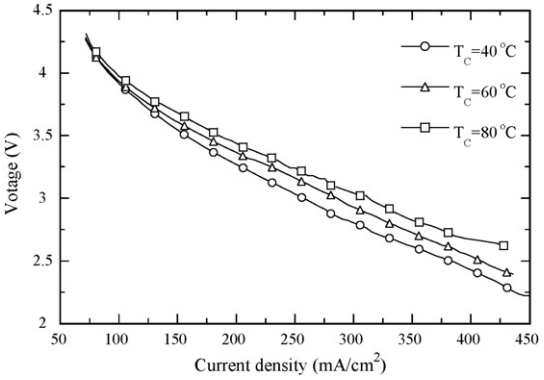

Fig. 5. Effect of cathode gas humidification temperature on the overall performance of the stack.

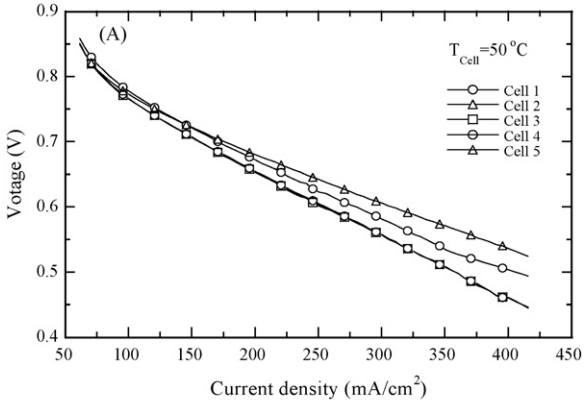

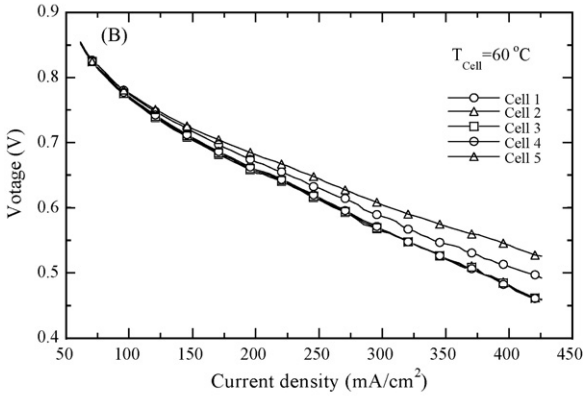

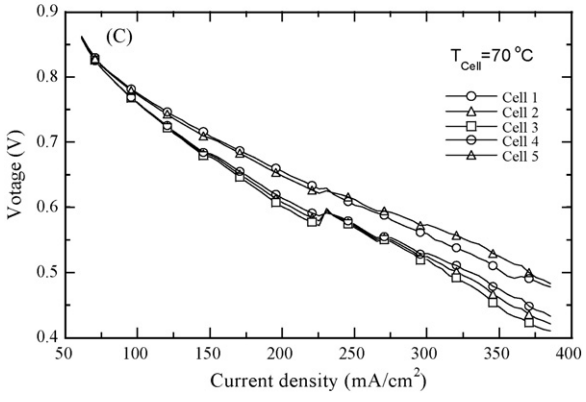

Fig. 6. Effect of cell temperature on the performance of each single cell's in the stack (A) 50 °C; (B) 60 °C; (C) 70 °C.

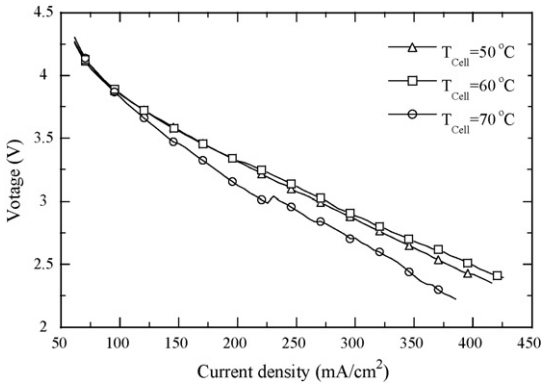

Fig. 7. Effect of cell temperature on the overall performance of the stack.

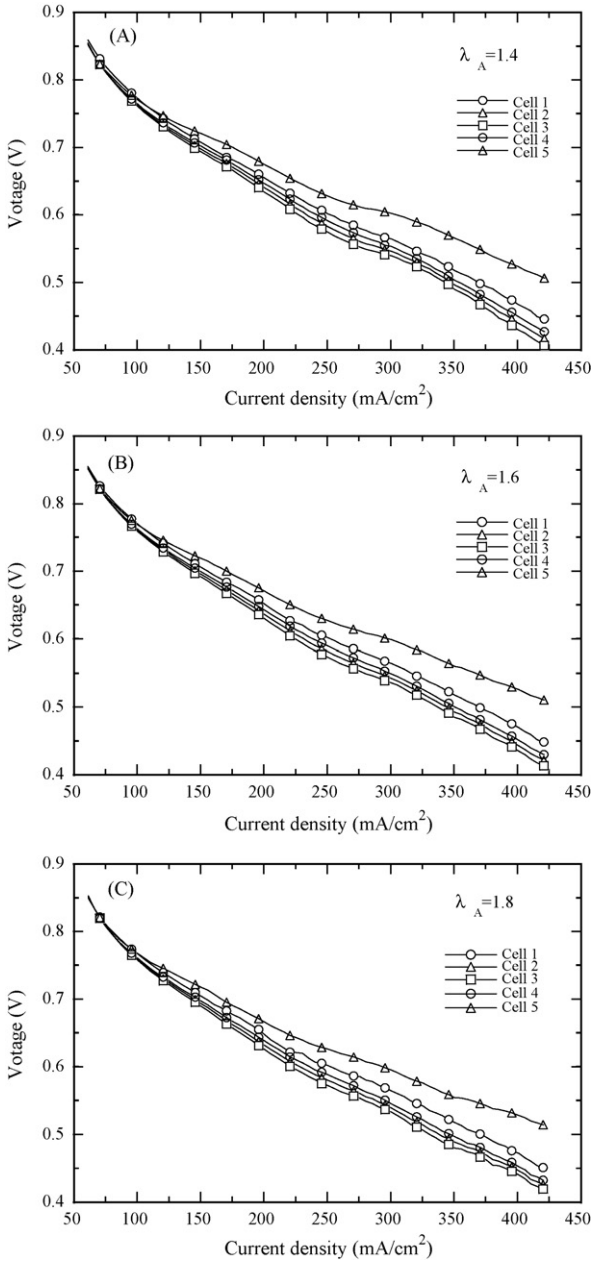

Fig. 8. Effect of anode gas stoichiometric ratio on the performance of each single cell in the stack; (A) $\lambda_A = 1.4$; (B) $\lambda_A = 1.6$; (C) $\lambda_A = 1.8$.

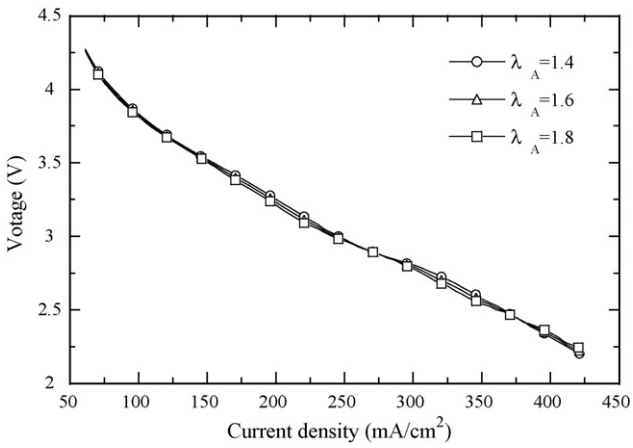

Fig. 9. Effect of anode gas stoichiometric ratio on the overall performance of the stack.

both anode and cathode are varied to investigate the parametric effects, such as humidification temperature, cell temperature, gas flow rate and assembling torsion. The effect of anode humidification temperature on the performances of each individual fuel cell is presented in Fig. 2. The cell temperature is fixed at 60 °C, and the stoichiometric ratio for both anode and cathode are 1.6 and 2.5, respectively. The assembling torsion is set at 70 lb in. It is seen that the performances for the cell on both sides are higher than those for the center cells in the stack. This is because the cells at the center are less humidified during operation. It is also noticed that the performances for each individual cell in the stack become closer as humidification temperature increases. The reason is that more humid in the fuel is delivered to the center cell, resulting in a decrease in the internal resistance of the center cell. However, the performances for the cells on both ends of the stack do not show a visible change with the increase of the anode humidification temperature. It is reasonable since the water content inside the cells on both ends of the stack is in saturated condition. Fig. 3 presents the effect of anode humidification temperature on the overall cell performance for the stack. It is clearly observed that the overall cell performance increases with the increase of anode humidification temperature. Apparently, the improved performance is beneficial with a better water management, especially for the cells near the center of the stack. The effects of cathode humidification temperature on the performances of individual cell and cell stack are presented in Figs. 4 and 5, respectively. Results similar to that for anode humidification temperature are obtained. The performances of individual cell and cell stack are improved as cathode humidification temperature increases. The improved performances are also a result from a better water management inside the cell stack by increasing cathode humidification temperature.

Figs. 6 and 7 represent the effects of cell temperature on the performance of individual cell and stack. In Fig. 6, results indicate that the difference between the performances for each cell in the cell stack is augmented as cell temperature increases. This can be explained by the fact that the relative humidity decreases as cell temperature increase, resulting in a drier condition for

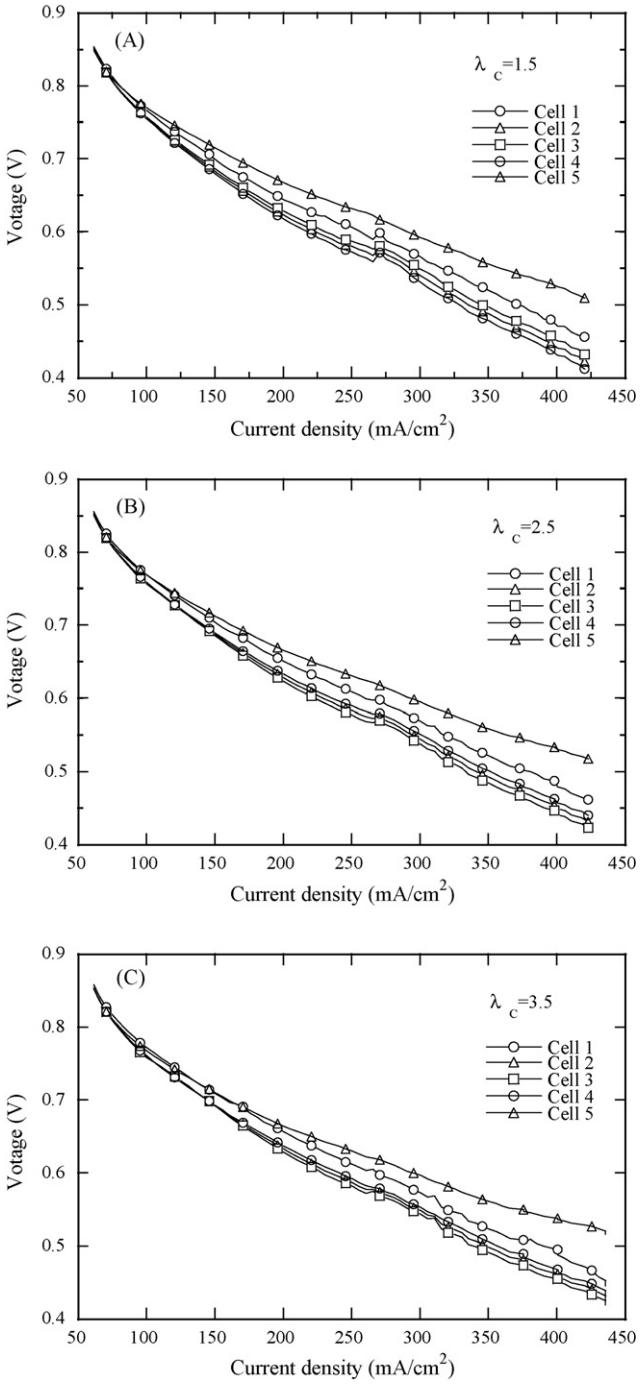

Fig. 10. Effect of cathode gas stoichiometric ratio on the performance of each single cell in the stack; (A) $\lambda_C = 1.5$; (B) $\lambda_C = 2.5$; (C) $\lambda_C = 3.5$.

the cells, especially for those at the center of the stack. However, the performances of cells on both ends of the cell stack do not show a visible difference with increasing cell temperature, because of sufficient supply of fuel and water. It is interesting to see in Fig. 7 that the overall performance with cell temperature of 60 °C is the best among the three cases. It can be easily understood that cell performance can be improved by increase of cell temperature resulting from an increase of internal energy and a decline of activation overpotential. However, when the cell temperature is up to 70 °C, the overall performance of the stack decreases, even lower than that of 50 °C. It is also observed in Fig. 6(C) that the performances for the cells at the center in the cell stack degraded for cell temperature to be 70 °C. This suggests that a proper cell temperature rise will be beneficial for the overall performance of the stack. This can be attributed to the low water content inside the stack at higher cell temperatures.

In this experiment, the effects of gas flow for both anode and cathode on the performance of individual cell and cell stack are also under investigation. The effects of anode gas stoichiometric ratio on the performance of individual cell and cell stack are presented in Figs. 8 and 9, respectively. It is clearly seen that the performances of individual cell and cell stack do not show a visible difference with the increase in anode gas stoichoimetric ratio. This is owing to the fact that sufficient fuel is supplied to individual cell, even for those at the center. As for the effect of cathode gas stoichiometric ratio, Figs. 10 and 11 indicate its influences on the performance of individual cell and cell stack, respectively. In Fig. 10, it is observed that the performances of each cell in stack are closer as cathode gas stoichiometric ratio increases. It is also seen in Fig. 10 that the performances of each cell in the stack are improved as a higher cathode gas stoichiometric ratio is used. This can be concluded that the oxidant is insufficient for the cells near center of the stack with lower cathode gas stoichiometric ratio. As the cathode gas stoichiometric ratio increases, the cell performance becomes better, especially for those at the center of the stack. In Fig. 11, the overall performance of the stack increases as cathode gas stoichiometric ratio increases. However, the improvement is not apparent even for $\lambda_C = 3.5$.

Assembling torsion is one of the important parameters for fuel cell stack, since the applied tension shall affect on the stress of each cell and gas leakage. The influences of assembling torsion of the stack on the performances of each single cell and cell stack are presented in Figs. 12 and 13, respectively. In Fig. 12, it is obvious to see that the performance of individual cell increases as assembling torsion increases. However, the performance differences between each cell are enlarged with

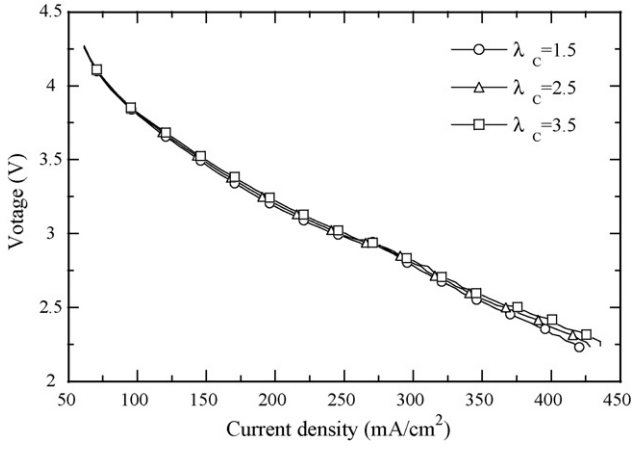

Fig. 11. Effect of cathode gas stoichiometric ratio on the overall performance of the stack.

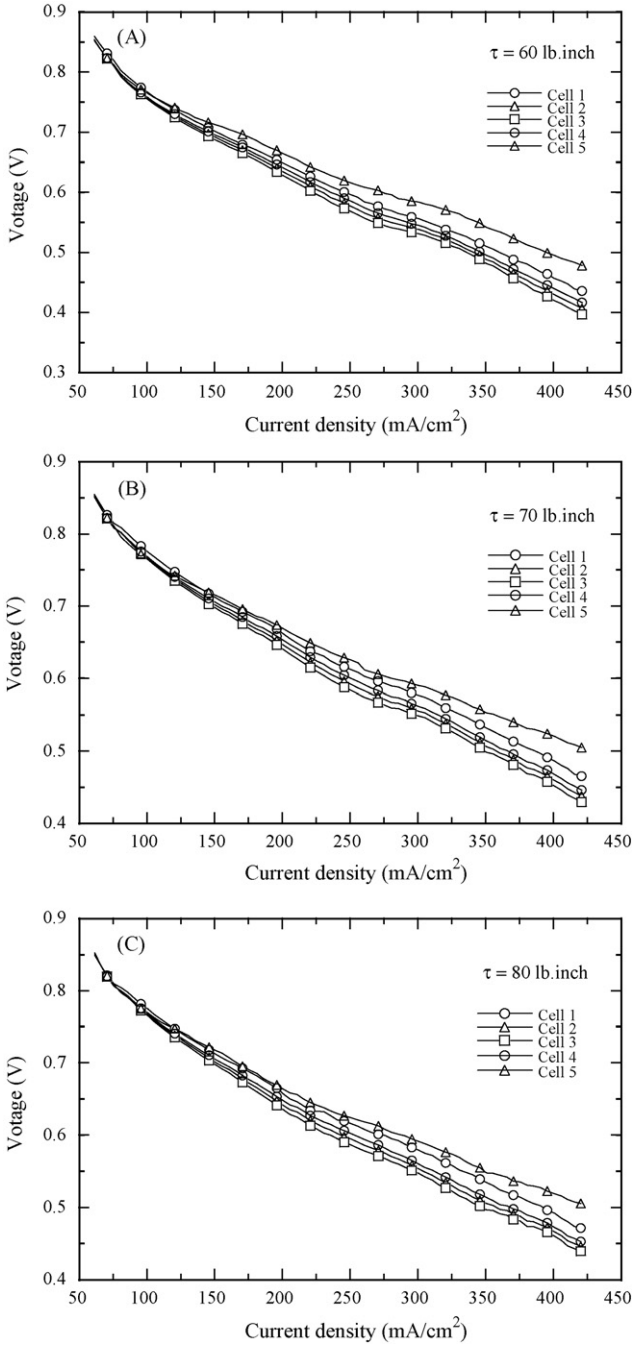

Fig. 12. Effect of assembling torsion on the performance of each single cell in the stack; (A) $\tau = 60$ lb in; (B) $\tau = 70$ lb in; (C) $\tau = 80$ lb in.

increase of assembling torsion. This means that the assembling torsion diminishes the internal contact resistance and gas leakage of each cell. As a result, the performance of each cell increases. In addition, the amount of increase in cell voltage decreases as assembling torsion increases. This will lead to an optimum performance for a specific assembling torsion value. Nevertheless, it is shown in Fig. 13 that the overall performance of the stack increases as the assembling torsion increases within the range of 60–80 lb in.

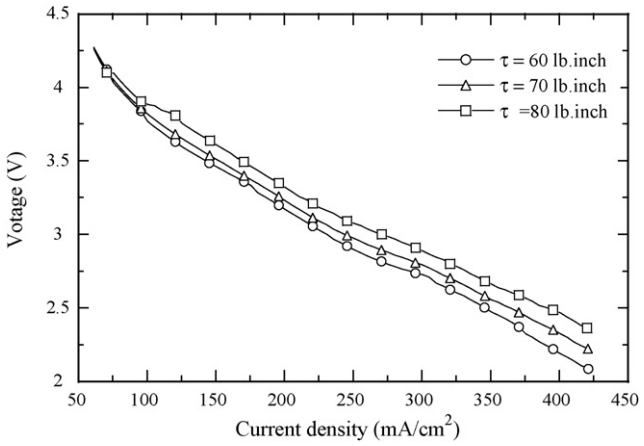

Fig. 13. Effect of assembling torsion on the overall performance of the stack.

4. Conclusion

In this experimental work, the influences of different operation parameters on the performances for each individual cell and cell stack of PEM fuel cell have been investigated. Operation parameters include anode humidification temperature, cell temperature, gas flow rate and assembling torsion. Conditions for both anode and cathode are considered. Based on the results, the following conclusions can be drawn.

1. Not only the individual cell, but also the overall stack shows better performance with increase of anode humidification temperature, especially for the cell at the center of the stack. Similar results are obtained for cathode.
2. The differences between performances of each cell in a stack are augmented as cell temperature increases. However, the overall performance of the stack can be improved with a proper raise of cell temperature.
3. Effects of anode gas stoichiometric ratio on the performances of individual cell and cell stack are not obvious; however, the performances of individual cell and cell stack are enlarged as cathode gas stoichiometric ratio increases.
4. The performances of each cell and cell stack increase as assembling torsion increases within the range of 60–80 lb in. The differences of performances for each cell in the stack are enlarged as assembling torsion increases.

Acknowledgement

The study was supported by the National Science Council, the Republic of China, through the grants NSC 93-2212-E-211-011 and NSC 95-2212-E-149-012. The financial support from Technology and Science Institute of Northern Taiwan is also appreciated.

References

[1] T.E. Springer, T.A. Zawodizinski, S. Gottesfeld, J. Electrochem. Soc. 138 (1991) 2334–2342.
[2] D.M. Bernardi, M.W. Verbrugge, AIChE J. 37 (1991) 1151–1163.
[3] T.V. Nguyen, R.E. White, J. Electrochem. Soc. 140 (1993) 2178–2186.

[4] T.F. Fuller, J. Newman, J. Electrochem. Soc. 140 (1993) 1218–1225.
[5] J.S. Yi, T.V. Nguyen, J. Electrochem. Soc. 145 (1998) 1149–1159.
[6] V. Gurau, H. Liu, S. Kakac, AIChE J. 44 (1998) 2410–2422.
[7] A. Kumar, R.G. Reddy, J. Power Sources 113 (2003) 11–18.
[8] F. Chen, Y.Z. Wen, H.S. Chu, W.M. Yan, C.Y. Soong, J. Power Sources 128 (2004) 125–134.
[9] S. Shimpalee, S. Greenway, D. Spuckler, J.W. Van Zee, J. Power Sources 135 (2004) 79–87.
[10] J.H. Jang, W.M. Yan, H.Y. Li, Y.C. Chou, J. Power Sources 159 (2006) 468–477.
[11] D.T.S. Rosa, D.G. Pinto, V.S. Silva, R.A. Silva, C.M. Rangel, Int. J. Hydrogen Energy 32 (2007) 4350–4357.
[12] W.L. Huang, Q. Zhu, J. Power Sources 178 (2008) 353–362.
[13] T.V. Nguyen, M.W. Knobbe, J. Power Sources 114 (2003) 70–79.
[14] G. Karimi, J.J. Baschuk, X. Li, J. Power Sources 147 (2005) 162–177.
[15] A.L.M. Reddy, S. Ramaprabhu, Int. J. Hydrogen Energy 32 (2007) 4272–4278.
[16] J. Chen, B. Zhou, J. Power Sources 177 (2008) 83–95.
[17] T. Mennola, M. Mikkola, M. Noponen, T. Hottinen, P. Lund, J. Power Sources 112 (2002) 261–272.
[18] S. Giddey, F.T. Ciacchi, S.P.S. Badwal, J. Power Sources 125 (2004) 155–165.
[19] W.H. Zhu, R.U. Payne, D.R. Cahela, B.J. Tatarchuk, J. Power Sources 128 (2004) 231–238.
[20] P. Rodatz, F. Buchi, C. Onder, L. Guzzella, J. Power Sources 128 (2004) 208–217.
[21] Y.J. Sohn, G.G. Park, T.H. Yang, Y.G. Yoon, W.Y. Lee, S.D. Yim, C.S. Kim, J. Power Sources 145 (2005) 604–609.
[22] T. Tanaka, K. Otsuka, K. Oyakawa, S. Watanabe, J. Power Sources 147 (2005) 208–213.
[23] D. Chu, R. Jiang, J. Power Sources 83 (1999) 128–133.
[24] M.W. Knobbe, W. He, P.Y. Chong, T.V. Nguyen, J. Power Sources 138 (2004) 94–100.
[25] X. Yan, M. Hou, L. Sun, D. Liang, Q. Shen, H. Xu, P. Ming, B. Yi, Int. J. Hydrogen Energy 32 (2007) 4358–4364.